CHARACTERIZATION OF NEW SYNTHESIZED Fe$_2$O$_3$ NANOPARTICLES AND THEIR APPLICATION AS DETECTION SIGNAL AMPLIFIERS IN HERBICIDE BENTAZONE ELECTROANALYTICAL DETERMINATION

ANJA JOKIĆ[1], BRANKA PETKOVIĆ[1], SONJA JEVTIĆ[1], VESNA VASIĆ[2], BOJANA LABAN[1*]

[1]Faculty of Natural Science and Mathematics, University of Priština, Kosovska Mitrovica, Serbia
[2]Vinča Institute of Nuclear Sciences, University of Belgrade, Belgrade, Serbia

ABSTRACT

The iron oxide nanoparticles (Fe$_2$O$_3$ NPs) were synthesized from two different iron salts by solid-state synthesis method. The synthesized powder of Fe$_2$O$_3$ NPs is soluble in water, and the colloidal dispersion was characterized by TEM, FTIR, UV-Vis spectroscopy and zeta potential measurements. Obtained NPs are spherical in shape with narrow particle size distribution and an average diameter of 3 nm. Further, the possible application of Fe$_2$O$_3$ NPs was proposed, due to significant electroanalytical signal amplification in the determination of herbicide bentazone in natural river water.

Keywords: Iron oxide, Nanoparticles, Solid-state, Herbicide bentazone, Electroanalysis.

INTRODUCTION

Nanotechnology is the field that has attracted attention over the past decade among many researches, because of multitude possibilities of nanoparticles (NPs) synthesis and/or their surface modification. Because of their small size, NPs have a large surface area-to-volume ratio, and due to that, they have enhanced surface chemistry. There are numerous studies and different methods of inorganic nanoparticles synthesis, both for metal and for metal oxides NPs, with different size, shape and surface coverage (Nguyen et al., 2006; Abdulwahab et al., 2014; Liao et al., 2010; Tang et al., 2006).

Iron NPs, zero-valent, and iron oxide, have gained considerable attention because of their unique physical, especially magnetic, and chemical properties (Sun et al., 2006; Ponder et al., 2001; Hasanzadeh et al., 2015), potential application in medicine (Ling et al., 2015; Zanganeh et al., 2016), and in drinking and/or wastewater treatment (Zhu et al., 2009; Rajput et al., 2016; Li et al., 2017). The iron and iron oxide NPs were previously synthesized using various methods, most often by co-precipitation, sol-gel, chemical reduction, etc. (Huang & Ehrman, 2007; Rani & Varma, 2015; Bashir et al., 2015; Sun et al., 2006; Lu et al., 2007). Further, surface modification of these NPs, in order to prevent their aggregation and/or agglomeration, and also with an aim to improve their surface properties, were reported (Sodipo & Aziz, 2016; Chen et al., 2017). Magnetic iron oxide NPs have been of considerable interest because of their use as sorbents of pesticides from water (Wu et al., 2011). There are two well-known phase of Fe$_2$O$_3$ NPs:

maghemite, the γ phase obtained at 300 °C, and hematite, the α phase obtained at 600 °C (Karami, 2010).

In this work, we report the synthesis of iron(III) oxide NPs by simple solid-state chemical reaction method, at room temperature, and in the air. The solid-state chemical reaction method presents a mechanochemical process where the chemical reaction occurs during grinding solid precursors. Application of this method provides a high yield of NPs. For Fe$_2$O$_3$ NPs synthesis two different iron salts were used as precursors.

As NPs and nanomaterials were recognized as excellent carriers and optical or electrical signal tags in sensing of biomolecules (Lei & Ju, 2012), the main idea of this work, besides obtaining monodisperse colloid dispersion, was also investigation of possibility of improvement in electroanalytical determination of pesticides, as serious environmental pollutants, due to amplification effect of NPs. Hence, previously synthesized Fe$_2$O$_3$ NPs obtained from different salts were used to enhance voltammetric response in determination of herbicide bentazone, one of the most frequently used herbicides in Europe, recently studied on boron doped diamond electrode by our research group (Jevtić et al., 2018).

EXPERIMENTAL

Reagents and standard solutions

Iron(II)-sulphate heptahydrate (FeSO$_4$·7H$_2$O), iron(III)-chloride hexahydrate (FeCl$_3$·6H$_2$O), potassium chloride (KCl) and potassium hydroxide (KOH), from Aldrich, were used as received. Stock solution of bentazone, 3-Isopropyl-1*H*-2,1,3-benzothiadiazin-4(3*H*)-one 2,2-dioxide (in further text presents with abbreviation BZ), 1×10^{-3} M was prepared in methanol. This compound was the product of Sigma –Aldrich. Britton Robinson

---

buffer (BR) was made from acetic, boric, and phosphoric acid (all 0.2 M) adjusted by sodium hydroxide to pH value 4. Water Purified Millipore Mili-Q with a resistivity of 18 MΩ was used for washing the reaction mixture.

Apparatus and measurements

Transmission electron microscopy (TEM) was used to estimate the shape and the average size of Fe_2O_3 NPs. TEM measurements were carried out using FEI Talos F200X at an operating voltage of 200 kV.

Absorption spectra of iron oxide colloidal dispersion were measured by Perkin Elmer Lambda 35 UV – Vis spectrophotometer using the quartz cuvette with 1cm path length.

FTIR spectra were measured by NICOLET I5 ATR spectrometer.
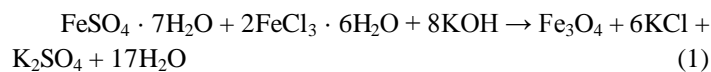
Zeta potential (ZP) measurements by laser Doppler electrophoresis (LDE) were performed using a Zeta-sizer Nano ZS with 633 nm He-Ne laser (Malvern Instruments, UK). Data were analyzed by the Zetasizer Software Version 6.20 (Malvern Instruments, UK).

Electrochemical measurements were performed at PalmSens 3 potentiostat/galvanostat/impedance analyzer with PSTrace software (PalmSens BV, Netherlands). Three electrode cell was consisted from CH Instruments reference Ag/AgCl electrode and counter Pt electrode, while boron-doped diamond electrode, BDDE, (Windsor Scientific Ltd, Slough, Berkshire, United Kingdom) was used as a working electrode for bentazone determination. DPV parameters were set as in our previous work (Jevtić et al., 2018). Differential pulse voltammetry (DPV) measurements were performed in solutions made as it follows: 2 ml of water from Serbian river Ibar was spiked with 1 ml of a colloidal suspension of synthesized Fe_2O_3 NPs (1.5 mg/10 ml) and proper volume of a standard solution of bentazone, and then fulfilled to 10 ml with BR buffer of pH 4.

RESULTS

Synthesis of iron oxide nanoparticles. Iron oxide NPs can be prepared by the solid-state method, via the chemical reaction between ferrous iron (Fe^{2+}) and/or ferric iron (Fe^{3+}) with the alkaline. In this work, we used two different iron salts, $FeSO_4 \cdot 7H_2O$ and $FeCl_3 \cdot 6H_2O$, in the molar ratio 1 : 2.5 (0.002 mol and 0.005mol). Iron salts were mixed in a mortar and ground for 30 min in air at room temperature; the yellow paste was obtained. The particle size and polydispersity of NPs can be tuned up by various factors (Ali et al., 2016), one of them is an ionic strength, so KCl is added in the reaction mixture to provide small NPs (Li et al., 2002). In yellow paste 0.02 mol of KOH was added to the mortar and grinded for the next 30 min. During grinding, yellow paste became dark brown to black and dry. The reaction mixture then was washed several times with purified water until SO_4^{2-} and Cl^- ions could not be detected. The advantage of this method is its simplicity, low cost, and

possibility to be done in every chemistry lab with simple chemical reagents. The chemical reaction goes on by the following equations:

$$FeSO_4 \cdot 7H_2O + 2FeCl_3 \cdot 6H_2O + 8KOH \rightarrow Fe_3O_4 + 6KCl + K_2SO_4 + 17H_2O \qquad (1)$$

$$4Fe_3O_4 + O_2 \rightarrow 6Fe_2O_3 \qquad (2)$$

In further work NPs were used as a powder or as a colloidal dispersion.

TEM characterization. The morphology and size of Fe_2O_3 NPs were determined from the diluted colloidal dispersion by TEM measurements. TEM micrograph along with particle size distribution are given in Fig. 1.
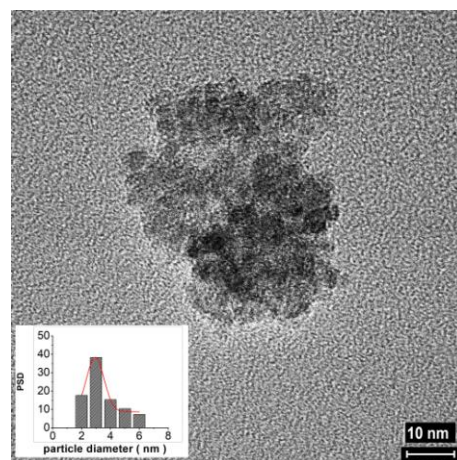

Figure 1. TEM micrograph of iron oxide NPs. Inset: Particle size distribution (PSD) of Fe_2O_3 NPs.

TEM measurements show that Fe_2O_3 NPs are spherical in shape with the average diameter of the particles of 2.9±0.07 nm. The mean particle size was obtained by fitting the TEM data with Gaussian distribution function (Fig. 1, inset).

Spectroscopic study. The absorption spectra of iron oxide colloidal dispersion contain broad absorption band around the area of 300 – 400 nm (Fig. 2.). Obtained data are in agreement with previously reported spectra for iron oxide colloids (Sayed and Polshettiwar, 2015).
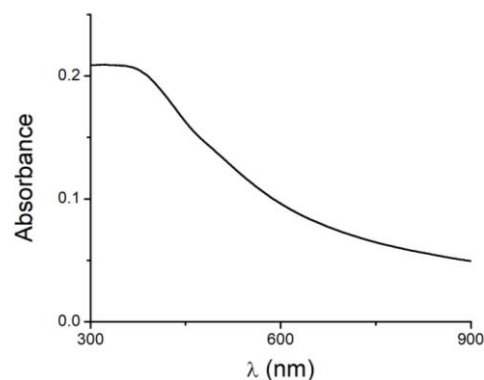

Figure 2. Absorption spectra of iron oxide colloidal dispersion.

Further, colloidal dispersion was left to dry in the air, at room temperature. Obtained powder of Fe_2O_3 NPs was than characterized by FTIR measurements. In FTIR spectrum, Fig. 3, the observed bands at 601 and 888 cm^{-1} are assigned to Fe – O stretching vibrations. The bands at 1640 and 3280 cm^{-1} are from bending and stretching vibrations of bonds in the molecule of water, which is present in a small amount in Fe_2O_3 NPs powder.
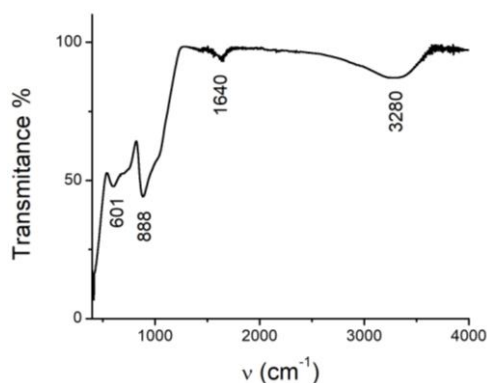

Figure 3. FTIR spectra of iron oxide NPs powder.

Zeta potential measurements. The charge of Fe_2O_3 NPs was determined by zeta potential measurements and shows that the surfaces of NPs are positively charged (+10 mV).

Electrochemistry of bentazone at BDDE in the presence of Fe_2O_3 NPs. Due to previously reported iron nanoparticles application as effective adsorbent material for wastewater and groundwater treatment of toxic contaminants (heavy metals, dyes etc.) (Chen et al., 2008; Saif et al., 2016), river water samples which contain different concentrations of herbicide bentazone were spiked with the synthesized and characterized Fe_2O_3 NPs. The content of BZ in river water samples were examined with previously reported electroanalytical method (Jevtić et al., 2018). Instead of the expected reduction of the voltammetric signal, it was found that the presence of Fe_2O_3 NPs in solution leads to a significant increase of DPV detection signal (Fig. 4). DPV voltammograms of river water samples without Fe_2O_3 NPs were also given in Fig.4 for comparison. As it can be seen, the peak potential for samples with Fe_2O_3 NPs was shifted to higher potentials probably due to interactions of molecules of BZ with the surface of Fe_2O_3 NPs. The main limitation of electroanalytical determination of bentazone represents instability of cation radical of BZ, its dimerization, and adsorption at the electrode (Manuela Garrido et al., 1998; Rahemi et al., 2013). The amplification of the detection signal may occur from the stabilization of cation radicals of bentazone due to interactions with Fe_2O_3 NPs. Nature of those interactions will be a subject of our further research.

Fig. 5 presents DPV voltammograms of BZ in the presence of Fe_2O_3 NPs in solution, recorded in the range of 5 to 90 μM of BZ, under the same experimental conditions and working DPV parameters as in our previous work (Jevtić et al., 2018).
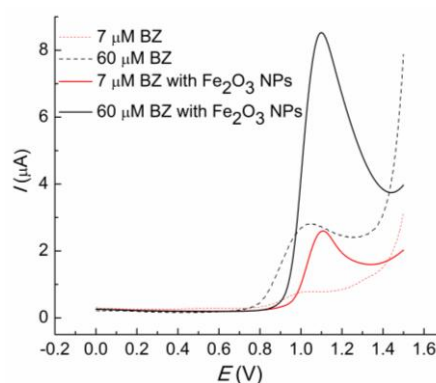

Figure 4. DPV voltammograms of different concentrations of BZ without and with Fe_2O_3 NPs in solution.
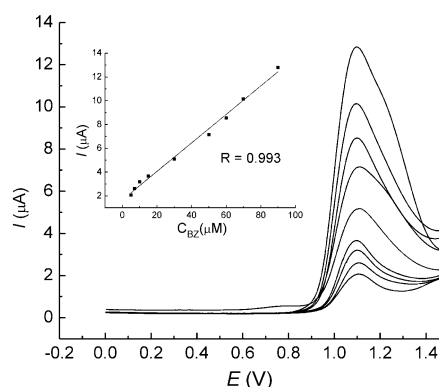

Figure 5. DPV voltammograms of different concentrations of BZ (5, 7, 10, 15, 30, 50, 60, 70, 90 μM) in BR buffer pH 4 at BDDE; Inset: Corresponding calibration curve.

The linear dependence expressed with the regression equation:

$$I\ (\mu A) = 1.660 + 0.119 \times C\ (\mu M);\ \ R = 0.993$$

was presented in the inserted graph in the same figure. The amplification of DPV signal of BZ in presence of Fe_2O_3 NPs also resulted in lowering of limit of detection (LOD) to the value of 0.09 μM.

Hence, the next task could be finding optimal experimental conditions and working parameters to achieve more sensitive determination of bentazone in presence of Fe_2O_3 NPs in solution, or even to employ Fe_2O_3 NPs as a modifier on the surface of the electrode.

CONCLUSION

Iron(III) oxide NPs were sucssesfuly synthesized by solid-state chemical reaction method from two different iron salts. The morphology characteristics show fine structured NPs, spherical in shape with a narrow distribution and an average diameter of ~3 nm. In electrochemical studies, Fe_2O_3 NPs show the amplifying effect on the voltammetric determination of herbicide bentazone at BDDE, offering interesting and promising results in

the application of these NPs in sensing of toxic materials and environmental pollutants.

ACKNOWLEGMENTS

REFERENCES

Abdulwahab, K. O., Malik, M. A., O'Brien, P., Timco, G. A., Tuna, F., Muryn, C. A., Winpenny, R. E. P., Pattrick, R. A. D., Coker, V. S., & Arenholz, E. 2014. A One-Pot Synthesis of Monodispersed Iron Cobalt Oxide and Iron Manganese Oxide Nanoparticles from Bimetallic Pivalate Clusters. Chemistry of Materials, 26(2), pp. 999-1013. doi:10.1021/cm403047v

Ali, A., Zafar, H., Zia, M., ul Haq, I., Phull, A. R., Ali, J. S., & Hussain, A. 2016. Synthesis, characterization, applications, and challenges of iron oxide nanoparticles. Nanotechnology, Science and Applications, Volume 9, pp. 49-67. doi:10.2147/nsa.s99986

Bashir, M., Riaz, S., & Naseem, S. 2015. Effect of pH on Ferromagnetic Iron Oxide Nanoparticles. Materials Today: Proceedings, 2(10), pp. 5664-5668. doi:10.1016/j.matpr.2015.11.106

Chen, K., He, J., Li, Y., Cai, X., Zhang, K., Liu, T., Hu, Y., Lin, D., Kong, L. & Liu, J. 2017. Removal of cadmium and lead ions from water by sulfonated magnetic nanoparticle adsorbents. Journal of Colloid and Interface Science, 494, pp. 307-316. doi:10.1016/j.jcis.2017.01.082

Chen, S. Y., Chen, W. H., & Shih, C. J. 2008. Heavy metal removal from wastewater using zero-valent iron nanoparticles. Water Science and Technology, 58(10), pp. 1947-1954. doi:10.2166/wst.2008.556

Garrido, M. E., Lima, C. J. L., Delerue-Matos, M. C. & Brett, M. O. A. 1998. Electrochemical oxidation of bentazon at a glassy carbon electrode: Application to the determination of a commercial herbicide. Talanta, 46, 1131-1135.

Hasanzadeh, M., Shadjou, N., & de la Guardia, M. 2015. Iron and iron-oxide magnetic nanoparticles as signal-amplification elements in electrochemical biosensing. TrAC Trends in Analytical Chemistry, 72, pp. 1-9. doi:10.1016/j.trac.2015.03.016

Huang, K., & Ehrman, S. H. 2007. Synthesis of Iron Nanoparticles via Chemical Reduction with Palladium Ion Seeds. Langmuir, 23(3), pp. 1419-1426. doi:10.1021/la0618364

Jevtić, S., Stefanović, A., Stanković, D. M., Pergal, M. V., Ivanović, A. T., Jokić, A., & Petković, B. B. 2018. Boron-doped diamond electrode — A prestigious unmodified carbon electrode for simple and fast determination of bentazone in river water samples. Diamond and Related Materials, 81, pp. 133-137. doi:10.1016/j.diamond.2017.12.009

Karami, H. 2010. Synthesis and Characterization of Iron Oxide Nanoparticles by Solid State Chemical Reaction Method. Journal of Cluster Science, 21(1), pp. 11-20. doi:10.1007/s10876-009-0278-x

Lei, J., & Ju, H. 2012. Signal amplification using functional nanomaterials for biosensing. Chemical Society Reviews, 41(6), p. 2122. doi:10.1039/c1cs15274b

Li, F., Xu, J., Yu, X., Chen, L., Zhu, J., Yang, Z., & Xin, X. 2002. One-step solid-state reaction synthesis and gas sensing property of tin oxide nanoparticles. Sensors and Actuators B: Chemical, 81(2-3), pp. 165-169. doi:10.1016/s0925-4005(01)00947-9

Li, S., Wang, W., Liang, F., & Zhang, W. 2017. Heavy metal removal using nanoscale zero-valent iron (nZVI): Theory and application. Journal of Hazardous Materials, 322, pp. 163-171. doi:10.1016/j.jhazmat.2016.01.032

Liao, Y., He, L., Huang, J., Zhang, J., Zhuang, L., Shen, H., & Su, C. 2010. Magnetite Nanoparticle-Supported Coordination Polymer Nanofibers: Synthesis and Catalytic Application in Suzuki-Miyaura Coupling. ACS Applied Materials & Interfaces, 2(8), pp. 2333-2338. doi:10.1021/am100354b

Ling, D., Lee, N., & Hyeon, T. 2015. Chemical Synthesis and Assembly of Uniformly Sized Iron Oxide Nanoparticles for Medical Applications. Accounts of Chemical Research, 48(5), pp. 1276-1285. doi:10.1021/acs.accounts.5b00038

Lu, J., Yang, S., Ng, K. M., Su, C., Yeh, C., Wu, Y., & Shieh, D. 2007. Solid-state synthesis of monocrystalline iron oxide nanoparticle based ferrofluid suitable for magnetic resonance imaging contrast application. Nanotechnology, 18(28), pp. 289001-289001. doi:10.1088/0957-4484/18/25/289001

Manuela, G. E., Costa, L. J. L., M. Delerue-Matos, C., & Maria, O. B. A. 1998. Electrochemical oxidation of bentazon at a glassy carbon electrodeApplication to the determination of a commercial herbicide. Talanta, 46(5), pp. 1131-1135. doi:10.1016/s0039-9140(97)00380-9

Nguyen, H. L., Howard, L. E. M., Stinton, G. W., Giblin, S. R., Tanner, B. K., Terry, I., Hughes, A. K., Ross, I. M., Serres, A. & Evans, J. S. O. 2006. Synthesis of Size-Controlled fcc and fct FePt Nanoparticles. Chemistry of Materials, 18(26), pp. 6414-6424. doi:10.1021/cm062127e

Ponder, S. M., Darab, J. G., Bucher, J., Caulder, D., Craig, I., Davis, L., Edelstein, N., Lukens, W., Nitsche, H., Rao, L., Shuh, D. K. & Mallouk, T. E. 2001. Surface Chemistry and Electrochemistry of Supported Zerovalent Iron Nanoparticles in the Remediation of Aqueous Metal Contaminants. Chemistry of Materials, 13(2), pp. 479-486. doi:10.1021/cm000288r

Rahemi, V., Garrido, J. M. P. J., Borges, F., Brett, C. M. A., & Garrido, E. M. P. J. 2013. Electrochemical Determination of the Herbicide Bentazone Using a Carbon Nanotube β-Cyclodextrin Modified Electrode. Electroanalysis, 25, pp. 2360-2366. doi:10.1002/elan.201300230

Rajput, S., Pittman, C. U., & Mohan, D. 2016. Magnetic magnetite (Fe 3 O 4) nanoparticle synthesis and applications for lead (Pb^{2+}) and chromium (Cr^{6+}) removal from water. Journal of Colloid and Interface Science, 468, pp. 334-346. doi:10.1016/j.jcis.2015.12.008

Rani, S., & Varma, G. D. 2015. Superparamagnetism and metamagnetic transition in Fe_3O_4 nanoparticles synthesized via co-precipitation method at different pH. Physica B: Condensed Matter, 472, pp. 66-77. doi:10.1016/j.physb.2015.05.016

Saif, S., Tahir, A., & Chen, Y. 2016. Green Synthesis of Iron Nanoparticles and Their Environmental Applications and

Implications. Nanomaterials, 6(11), p. 209. doi:10.3390/nano6110209

Sayed, F. N., & Polshettiwar, V. 2015. Facile and Sustainable Synthesis of Shaped Iron Oxide Nanoparticles: Effect of Iron Precursor Salts on the Shapes of Iron Oxides. Scientific Reports, 5(1). doi:10.1038/srep09733

Sodipo, B. K., & Aziz, A. A. 2016. Recent advances in synthesis and surface modification of superparamagnetic iron oxide nanoparticles with silica. Journal of Magnetism and Magnetic Materials, 416, pp. 275-291. doi:10.1016/j.jmmm.2016.05.019

Sun, Y., Li, X., Cao, J., Zhang, W., & Wang, H. P. 2006. Characterization of zero-valent iron nanoparticles. Advances in Colloid and Interface Science, 120(1-3), pp. 47-56. doi:10.1016/j.cis.2006.03.001

Tang, B., Wang, G., Zhuo, L., Ge, J., & Cui, L. 2006. Facile Route to α-FeOOH and α-Fe$_2$O$_3$ Nanorods and Magnetic Property of α-Fe$_2$O$_3$ Nanorods. ChemInform, 37(38). doi:10.1002/chin.200638198

Wu, Q., Zhao, G., Feng, C., Wang, C., & Wang, Z. 2011. Preparation of a graphene-based magnetic nanocomposite for the extraction of carbamate pesticides from environmental water samples. Journal of Chromatography A, 1218(44), pp. 7936-7942. doi:10.1016/j.chroma.2011.09.027

Zanganeh, S., Hutter, G., Spitler, R., Lenkov, O., Mahmoudi, M., Shaw, A., Pajarinen, J. S., Nejadnik, H., Goodman, S., Moseley, M., Coussens, L. M. & Daldrup-Link, H. E. 2016. Iron oxide nanoparticles inhibit tumour growth by inducing pro-inflammatory macrophage polarization in tumour tissues. Nature Nanotechnology, 11(11), pp. 986-994. doi:10.1038/nnano.2016.168

Zhu, H., Jia, Y., Wu, X., & Wang, H. 2009. Removal of arsenic from water by supported nano zero-valent iron on activated carbon. Journal of Hazardous Materials, 172(2-3), pp. 1591-1596. doi:10.1016/j.jhazmat.2009.08.031